Chemostat Model Analysis with Different Kernels and Fractional Derivatives

Ali Akgül[1,2,3,*], Enver Ülgül[2], Rubayyi T. Alqahtani[4]

[1]*Department of Computer Science and Mathematics, Lebanese American University, Beirut, Lebanon*

[2]*Siirt University, Art and Science Faculty, Department of Mathematics, TR-56100 Siirt, Turkey*

[3]*Near East University, Mathematics Research Center, Department of Mathematics, Near East Boulevard, PC: 99138, Nicosia /Mersin 10 – Turkey; aliakgul00727@gmail.com*

[4]*Department of Mathematics and Statistics, College of Science, Imam Mohammad Ibn Saud Islamic University (IMSIU), Riyadh 11432, Saudi Arabia*

Abstract

Three ordinary differential equations are used to represent mathematically the breakdown of a phenol and p-cresol combination in a constantly agitated bioreactor.The research offers a stability analysis of the model's equilibrium locations. Three different kernels have also been used to examine the effects of the fractal dimension and the fractional order on the model with the fractal-fractional derivatives. We have developed extremely effective computational techniques for phenol, p-cresol, and biomass concentrations. Finally, computer simulations are used to confirm the correctness of the suggested strategy.

Keywords: Bioreactor Model; Computational Methods, Fractal-Fractional Derivatives, Computational Simulations.

1. Introduction

There are numerous scientific articles that describe the discovery and work of microbial species that have greater chemical compound degradation activity [1]. Numerous individual microorganisms have been studied in [2]. The nature of the particular mixture and the used microbes determine whether one or all chemical components will biodegrade [3, 4, 5, 6]. FThe classical derivatives have a significant extension in fractional calculus. Fractional differential equations (FDEs) have recently been used in a variety of disciplines. Many authors have worked on these equations such as KdV equation [7], advection-dispersion equation [8], telegraph equation [9], Schrodinger equation [10], heat equation [11], convection diffusion

*Corresponding author.

Email addresses: aliakgul@siirt.edu.tr (Ali Akgül[1,2,3,*]), enverulgul0244@hotmail.com (Enver Ülgül[2]), rtalqahtani@imamu.edu.sa (Rubayyi T. Alqahtani[4])

equation [12], Fokker Planck equation [13]. Some of the FDEs do not have exact solution, therefore it is required to work on computational methods to solve the mentioned equations such as solving nonlinear fractional diffusion wave equation with homotopy analysis technique [14], solving PDEs of fractal order by Adomian decomposition method [15]. In [1], the authors have given a bioreactor model but they do not consider the death rate of bacteria and also general configuration of the reactor. We have provided the bioreactor model with the fractal-fractional derivatives (FFD). The model with fractal-fractional derivatives has never been analysed so far. Our model includes the death rate of bacteria which is important in environment of the process. We also consider general configuration of the reactor where our model includes a membrane and continuous reactor. Additionally, we fractionalize the model and apply a novel computational technique to get the computational simulations.

We organize our manuscript as follow. Problem formulation is done in Section 2. In Section 3 we have discussed the analysis of the model in the classical case and presented the equilibria and stability analysis. Sections 4, 5 and 6 deals with analysis of the model with three different kernels viz the power-law kernel, the exponential-decay kernel and the Mittag-Leffler kernel respectively and in section 7 we demonstrate the computational simulations.

2. Preliminaries

The following definitions of FFD and fractal-fractional integral (FFI) with three different kernels are taken from [16] .

Definition 2.1. *The FFD with power-law type kernel is described as:*

$$ {}_{c}^{FFP}D_{t}^{\alpha,\eta} f(t) = \frac{1}{1-\alpha}\frac{d}{du^{\eta}}\int_{c}^{t} f(s)(t-s)^{-\alpha}ds,\ 0<\alpha,\eta\leq 1, \tag{1} $$

where,

$$ \frac{df(s)}{ds^{\eta}} = \lim_{t\to s}\frac{f(t)-f(s)}{t^{\eta}-s^{\eta}} \tag{2} $$

Definition 2.2. *The FFD with exponential-decay type kernel is described as:*

$$ {}_{c}^{FFE}D_{t}^{\alpha,\eta} f(t) = \frac{M_1(\alpha)}{1-\alpha}\frac{d}{dt^{\eta}}\int_{c}^{t} f(s)\exp\Big(\frac{-\alpha}{1-\alpha}(t-s)\Big)ds,\ 0<\alpha,\eta\leq 1. \tag{3} $$

Definition 2.3. *The FFD with Mittag-Leffler type kernel is described as:*

$$ {}_{c}^{FFM}D_{t}^{\alpha,\eta} f(t) = \frac{AB(\alpha)}{1-\alpha}\frac{d}{dt^{\eta}}\int_{c}^{t} f(s)E_{\alpha}\Big(\frac{-\alpha}{1-\alpha}(t-s)^{\alpha}\Big)ds,\ 0<\alpha,\eta\leq 1, \tag{4} $$

where, $AB(\alpha) = 1-\alpha+\frac{\alpha}{\Gamma(\alpha)}$.

Definition 2.4. *The FFI with power-law type kernel is described as:*

$$ {}_{0}^{FFP}I_{t}^{\alpha,\eta} f(t) = \frac{\eta}{\Gamma(\alpha)}\int_{0}^{t}(t-s)^{\alpha-1}s^{\tau-1}\phi(s)ds. \tag{5} $$

Definition 2.5. *The FFI with exponential-decay type kernel is described as:*

$$ {}_{0}^{FFE}I_{t}^{\alpha,\eta} f(t) = \frac{\alpha\eta}{M_1(\alpha)}\int_{0}^{t}s^{\alpha-1}f(s)ds + \frac{\tau(1-\alpha)t^{\tau-1}}{M_1(\alpha)}\phi(t). \tag{6} $$

Definition 2.6. *The FFI with Mittag-Leffler type kernel is described as:*

$$ {}_{0}^{FFM}I_{t}^{\alpha,\eta} f(t) = \frac{\alpha\eta}{AB(\alpha)}\int_{0}^{t}s^{\alpha-1}f(s)(t-s)^{\alpha-1}ds + \frac{\tau(1-\alpha)t^{\tau-1}}{AB(\alpha)}f(t). \tag{7} $$

3. Formation of the model

Here, we provide the model that will be examined in this study. The three-dimensional model is provided as follows:

$$ \frac{\mathrm{d}S_{ph}}{\mathrm{d}t} = D\left(S_{ph0}-S_{ph}\right) - k_{ph}\cdot\mu\left(S_{ph},S_{cr}\right)\cdot X, \tag{8} $$

$$ \frac{\mathrm{d}S_{cr}}{\mathrm{d}t} = D\left(S_{cr0}-S_{cr}\right) - k_{cr}\cdot\mu\left(S_{ph},S_{cr}\right)\cdot X, \tag{9} $$

$$ \frac{\mathrm{d}X}{\mathrm{d}t} = -D\beta X + \mu\left(S_{ph},S_{cr}\right)X, \tag{10} $$

$$ \mu\left(S_{ph},S_{cr}\right) = \frac{\mu_{max(ph)}S_{ph}}{K_{s(ph)}+S_{ph}+\frac{S_{ph}^{2}}{k_{i(ph)}}+I_{cr/ph}S_{cr}} + \frac{\mu_{max(cr)}S_{cr}}{K_{s(cr)}+S_{cr}+\frac{S_{cr}^{2}}{k_{i(cr)}}+I_{ph/cr}S_{ph}}, \tag{11} $$

The model parameters and variables are detailed in [1]. The parameter β is presented in the general configuration. When $\beta = 1$ we have continued the reactor. When $\beta = 0$ we have a membrane reactor.

4. Analysis of the model in classical sense

We will now start by performing a traditional analysis of the model's attributes.

4.1. Equilibria and Stability analysis

We take into account how many model (8- 10) equilibrium solutions there are. The model clearly has a branch of the washout specified by: ,

$$E_0 = (S_{ph}, S_{cr}, X) = \left(S_{ph0}, S_{cr0}, 0\right). \tag{12}$$

We obtain the steady state solution of (8- 10) by setting to zero the right side. From the model (8- 10), we have,

$$\begin{aligned} S_{cr} &= \frac{S_{cr0}k_{ph} + k_{cr}(S_{ph} - S_{ph0})}{k_{ph}}, \\ X &= \frac{D\left(S_{ph0} - S_{ph}\right)}{k_{ph}\ (\beta D)}. \end{aligned} \tag{13}$$

$$f = \begin{pmatrix} -k_{cr}\mu(s_{ph},s_{cr})X \\ \mu(s_{ph},s_{cr})X \end{pmatrix} \quad \rightarrow \quad F = \begin{bmatrix} \frac{\partial\mu(s_{ph},s_{cr})(-k_{cr})X}{\partial(s_{ph},s_{cr})X} & -k_{cr}\mu(s_{ph}, s_{cr}) \\ \\ \frac{\partial\mu(s_{ph},s_{cr})X}{\partial(s_{ph},s_{cr})X} & \mu(s_{ph}, s_{cr})k_{cr}(s_{ph}, s_{cr}) \end{bmatrix}$$

$$V = \begin{pmatrix} -D(s_{cr0} - s_{cr}) \\ D\beta X \end{pmatrix} \quad \rightarrow \quad V = \begin{bmatrix} D & 0 \\ \\ 0 & D\beta \end{bmatrix} \ , V^{-1} = \begin{bmatrix} D\beta & 0 \\ \\ 0 & D \end{bmatrix}$$

$$FV^{-1} = \begin{bmatrix} 0 & -k_{cr}\mu(s_{ph}, s_{cr}) \\ \\ 0 & \mu(s_{ph}, s_{cr}) \end{bmatrix} \begin{bmatrix} D & 0 \\ \\ 0 & D\beta \end{bmatrix} = \begin{bmatrix} 0 & -Dk_{cr}\mu(s_{ph}, s_{cr}) \\ \\ 0 & D\mu(s_{ph}, s_{cr}) \end{bmatrix}$$

$$det\left[\ FV^{-1} - \lambda I_2\ \right] = 0 \quad , \begin{vmatrix} -\lambda & -Dk_{cr}\mu(s_{ph}, s_{cr}) \\ \\ 0 & D\mu(s_{ph}, s_{cr}) - \lambda \end{vmatrix} = 0$$

Thus, we obtain $\lambda_1 = 0, \quad \lambda_2 = D\mu(s_{ph}, s_{cr}) = R_0$

Lemma 4.0.1. *The steady state solution E_0 is locally asymptotically stable when $D > D_{cr}$ and is unstable when $D < D_{cr}$.*

Proof. We have

$$E_0 = (s_{ph}, s_{cr}, x) = (s_{ph0}, s_{cr0}, 0)$$

$$J(E_0) = \begin{bmatrix} -D - \frac{\partial \mu(s_{ph}, s_{cr})}{\partial s_{ph}} k_{ph} x & -\frac{\partial \mu(s_{ph}, s_{cr})}{\partial s_{ph}} k_{ph} x & -\mu(s_{ph}, s_{cr}) k_{ph} \\ -k_{cr} \frac{\partial \mu(s_{ph}, s_{cr})}{\partial s_{ph}} x & -D - \frac{\partial \mu(s_{ph}, s_{cr})}{\partial s_{ph}} k_{cr} x & -\mu(s_{ph}, s_{cr}) k_{cr} \\ \frac{\partial \mu(s_{ph}, s_{cr})}{\partial s_{ph}} x & -\frac{\partial \mu(s_{ph}, s_{cr})}{\partial s_{ph}} x & -D\beta + \mu(s_{ph}, s_{cr}) \end{bmatrix}$$

$$J(E_0) = \begin{bmatrix} -D & 0 & -\mu(s_{ph0}, s_{cr0}) k_{ph} \\ 0 & -D & -\mu(s_{ph0}, s_{cr0}) k_{cr} \\ 0 & 0 & -D\beta + \mu(s_{ph0}, s_{cr0}) \end{bmatrix}$$

where

$$\mu(s_{ph}, s_{cr}) = \frac{\mu_{max(ph)} s_{ph}}{K_{s(ph)} + s_{ph} + \frac{s_{ph}^2}{K_{i(ph)}} + I_{cr/ph} s_{cr}} + \frac{\mu_{max(cr)} s_{ph}}{K_{s(cr)} + s_{cr} + \frac{s_{cr}^2}{K_{i(cr)}} + I_{ph/cr} s_{ph}}$$

$$\det[J(E_0) - \lambda I_3] = \begin{vmatrix} -D - \lambda & 0 & -\mu(s_{ph}, s_{cr}) k_{ph} \\ 0 & -D - \lambda & -\mu(s_{ph}, s_{cr}) k_{cr} \\ 0 & 0 & \mu(s_{ph}, s_{cr}) - D\beta - \lambda \end{vmatrix} = 0$$

$$= (-D - \lambda)(-D - \lambda)(\mu(s_{ph}, s_{cr}) - D\beta - \lambda) = 0$$

$$\lambda_1 = -D, \quad \lambda_2 = -D, \quad \lambda_3 = -\beta D + \mu(s_{ph}, s_{cr})$$

and

$$\mu(s_{ph}, s_{cr}) = ^{-} max_{ph} s_{ph0} (k_{sph} + s_{ph0} + \frac{s_{ph0}^2}{K_{i(ph)}} + I_{cr/ph} s_{cr0})^{-1}$$
$$+ ^{-} max_{cr} s_{cr0} (k_{scr} + s_{cr0} + \frac{s_{cr0}^2}{K_{i(ph)}} + I_{ph/cr} s_{ph0})^{-1}$$
$$D_{cr} = \frac{k_{icr} k_{ph} (s_{cr0} k_{ph} - s_{ph0} k_{cr})^{-} max_{cr}}{\left[k_{icr} k_{ph} (K_{scr} k_{ph} + s_{cr0} k_{ph} - s_{ph0} k_{cr}) + (s_{cr} k_{ph} - s_{ph0} k_{cr})^2 \right] \beta}$$

If $D > D_{cr}$, then $\lambda_3 < 0$. Thus, all eigenvalues are negative. This presents that the steady state solution E_0 is locally asymptotically stable. □

5. Analysis of the Model with the Power-Law Kernel

Here we analyze the model with FFD using the power-law kernel as:

$$ {}_0^{FFP}D_t^{\alpha,\eta} S_{ph} = D\left(S_{ph0} - S_{ph}\right) - k_{ph} \cdot \mu\left(S_{ph}, S_{cr}\right) \cdot X, \tag{14} $$

$$ {}_0^{FFP}D_t^{\alpha,\eta} S_{cr} = D\left(S_{cr0} - S_{cr}\right) - k_{cr} \cdot \mu\left(S_{ph}, S_{cr}\right) \cdot X, \tag{15} $$

$$ {}_0^{FFP}D_t^{\alpha,\eta} X = -D\beta X + \mu\left(S_{ph}, S_{cr}\right) X \tag{16} $$

We have [16]:

$$ D^{\eta} f(t) = \frac{f'(t)}{\eta t^{\eta-1}}. \tag{17} $$

Then, we acquire

$$ {}_0^{RL}D_t^{\alpha} S_{ph} = \eta t^{\eta-1}\left(D\left(S_{ph0} - S_{ph}\right) - k_{ph} \cdot \mu\left(S_{ph}, S_{cr}\right) \cdot X\right), \tag{18} $$

$$ {}_0^{RL}D_t^{\alpha} S_{cr} = \eta t^{\eta-1}\left(D\left(S_{cr0} - S_{cr}\right) - k_{cr} \cdot \mu\left(S_{ph}, S_{cr}\right) \cdot X\right), \tag{19} $$

$$ {}_0^{RL}D_t^{\alpha} X = \eta t^{\eta-1}\left(-D\beta X + \mu\left(S_{ph}, S_{cr}\right) X\right) \tag{20} $$

For simplicity, we define

$$ A(t, S_{ph}, S_{cr}, X) = \eta t^{\eta-1}\left(D\left(S_{ph0} - S_{ph}\right) - k_{ph} \cdot \mu\left(S_{ph}, S_{cr}\right) \cdot X\right), \tag{21} $$

$$ B(t, S_{ph}, S_{cr}, X) = \eta t^{\eta-1}\left(D\left(S_{cr0} - S_{cr}\right) - k_{cr} \cdot \mu\left(S_{ph}, S_{cr}\right) \cdot X\right), \tag{22} $$

$$ C(t, S_{ph}, S_{cr}, X) = \eta t^{\eta-1}\left(-D\beta X + \mu\left(S_{ph}, S_{cr}\right) X\right) \tag{23} $$

Then, we obtain

$$ {}_0^{RL}D_t^{\alpha} S_{ph} = A(t, S_{ph}, S_{cr}, X) \tag{24} $$

$$ {}_0^{RL}D_t^{\alpha} S_{cr} = B(t, S_{ph}, S_{cr}, X) \tag{25} $$

$$ {}_0^{RL}D_t^{\alpha} X = C(t, S_{ph}, S_{cr}, X) \tag{26} $$

Applying the Riemann-Liouville integral yields:

$$S_{ph}(t) - S_{ph}(0) = \frac{1}{\Gamma(\alpha)} \int_0^t A(\tau, S_{ph}, S_{cr}, X)(t-\tau)^{\alpha-1} d\tau \tag{27}$$

$$S_{cr}(t) - S_{cr}(0) = \frac{1}{\Gamma(\alpha)} \int_0^t B(\tau, S_{ph}, S_{cr}, X)(t-\tau)^{\alpha-1} d\tau \tag{28}$$

$$X(t) - X(0) = \frac{1}{\Gamma(\alpha)} \int_0^t C(\tau, S_{ph}, S_{cr}, X)(t-\tau)^{\alpha-1} d\tau \tag{29}$$

Discretizing the above equations at t_{n+1}, we get:

$$S_{ph}(t_{n+1}) - S_{ph}(0) = \frac{1}{\Gamma(\alpha)} \int_0^{t_{n+1}} A(\tau, S_{ph}, S_{cr}, X)(t_{n+1}-\tau)^{\alpha-1} d\tau \tag{30}$$

$$S_{cr}(t_{n+1}) - S_{cr}(0) = \frac{1}{\Gamma(\alpha)} \int_0^{t_{n+1}} B(\tau, S_{ph}, S_{cr}, X)(t_{n+1}-\tau)^{\alpha-1} d\tau \tag{31}$$

$$X(t_{n+1}) - X(0) = \frac{1}{\Gamma(\alpha)} \int_0^{t_{n+1}} C(\tau, S_{ph}, S_{cr}, X)(t_{n+1}-\tau)^{\alpha-1} d\tau \tag{32}$$

$$S_{ph}(t_{n+1}) - S_{ph}(0) = \frac{1}{\Gamma(\alpha)} \sum_{j=0}^{n} \int_{t_j}^{t_{j+1}} A(\tau, S_{ph}, S_{cr}, X)(t_{n+1}-\tau)^{\alpha-1} d\tau \tag{33}$$

$$S_{cr}(t_{n+1}) - S_{cr}(0) = \frac{1}{\Gamma(\alpha)} \sum_{j=0}^{n} \int_{t_j}^{t_{j+1}} B(\tau, S_{ph}, S_{cr}, X)(t_{n+1}-\tau)^{\alpha-1} d\tau \tag{34}$$

$$X(t_{n+1}) - X(0) = \frac{1}{\Gamma(\alpha)} \sum_{j=0}^{n} \int_{t_j}^{t_{j+1}} C(\tau, S_{ph}, S_{cr}, X)(t_{n+1}-\tau)^{\alpha-1} d\tau \tag{35}$$

Two-step Lagrange polynomial is used as:

$$p_j(\tau, S_{ph}, S_{cr}, X) = \frac{\tau - t_{j-1}}{t_j - t_{j-1}} A(t_j, S_{ph}, S_{cr}, X) - \frac{\tau - t_j}{t_j - t_{j-1}} A(t_{j-1}, S_{ph}, S_{cr}, X) \tag{36}$$

$$q_j(\tau, S_{ph}, S_{cr}, X) = \frac{\tau - t_{j-1}}{t_j - t_{j-1}} B(t_j, S_{ph}, S_{cr}, X) - \frac{\tau - t_j}{t_j - t_{j-1}} B(t_{j-1}, S_{ph}, S_{cr}, X) \tag{37}$$

$$s_j(\tau, S_{ph}, S_{cr}, X) = \frac{\tau - t_{j-1}}{t_j - t_{j-1}} C(t_j, S_{ph}, S_{cr}, X) - \frac{\tau - t_j}{t_j - t_{j-1}} C(t_{j-1}, S_{ph}, S_{cr}, X) \tag{38}$$

Then, we obtain

$$
\begin{aligned}
S_{ph}(t_{n+1}) - S_{ph}(0) = & \frac{1}{\Gamma(\alpha)} \sum_{j=0}^{n} \int_{t_j}^{t_{j+1}} p(\tau, S_{ph}, S_{cr}, X)(t_{n+1} - \tau)^{\alpha-1} d\tau \\
= & \sum_{j=0}^{n} \left[\frac{h^\alpha A(t_j, S_{ph}, S_{cr}, X)}{\Gamma(\alpha+2)} \left((n+1-j)^\alpha (n-j+2+\alpha) \right. \right. \\
& \left. \left. -(n-j)^\alpha (n-j+2+2\alpha) \right) \right] \\
& - \sum_{j=0}^{n} \left[\frac{h^\alpha A(t_{j-1}, S_{ph}, S_{cr}, X)}{\Gamma(\alpha+2)} \left((n+1-j)^{\alpha+1} \right. \right. \\
& \left. \left. -(n-j)^\alpha (n-j+1+\alpha) \right) \right]
\end{aligned}
$$

$$
\begin{aligned}
S_{cr}(t_{n+1}) - S_{cr}(0) = & \frac{1}{\Gamma(\alpha)} \sum_{j=0}^{n} \int_{t_j}^{t_{j+1}} q(\tau, S_{ph}, S_{cr}, X)(t_{n+1} - \tau)^{\alpha-1} d\tau \\
= & \sum_{j=0}^{n} \left[\frac{h^\alpha B(t_j, S_{ph}, S_{cr}, X)}{\Gamma(\alpha+2)} \left((n+1-j)^\alpha (n-j+2+\alpha) \right. \right. \\
& \left. \left. -(n-j)^\alpha (n-j+2+2\alpha) \right) \right] \\
& - \sum_{j=0}^{n} \left[\frac{h^\alpha B(t_{j-1}, S_{ph}, S_{cr}, X)}{\Gamma(\alpha+2)} \left((n+1-j)^{\alpha+1} \right. \right. \\
& \left. \left. -(n-j)^\alpha (n-j+1+\alpha) \right) \right]
\end{aligned}
$$

$$
\begin{aligned}
X(t_{n+1}) - X(0) = & \frac{1}{\Gamma(\alpha)} \sum_{j=0}^{n} \int_{t_j}^{t_{j+1}} s(\tau, S_{ph}, S_{cr}, X)(t_{n+1} - \tau)^{\alpha-1} d\tau \\
= & \sum_{j=0}^{n} \left[\frac{h^\alpha C(t_j, S_{ph}, S_{cr}, X)}{\Gamma(\alpha+2)} \left((n+1-j)^\alpha (n-j+2+\alpha) \right. \right. \\
& \left. \left. -(n-j)^\alpha (n-j+2+2\alpha) \right) \right] \\
& - \sum_{j=0}^{n} \left[\frac{h^\alpha C(t_{j-1}, S_{ph}, S_{cr}, X)}{\Gamma(\alpha+2)} \left((n+1-j)^{\alpha+1} \right. \right. \\
& \left. \left. -(n-j)^\alpha (n-j+1+\alpha) \right) \right]
\end{aligned}
$$

Thus, the computational scheme for the model with power law kernel has been obtained. We used this scheme and obtained Figures 1-4.

6. Analysis of the Model with the Exponential-Decay Kernel

Next we analyze the model with FFD using the exponential-decay kernel as:

$$ {}_{0}^{FFE}D_{t}^{\alpha,\eta}S_{ph} = D\left(S_{ph0} - S_{ph}\right) - k_{ph}\cdot\mu\left(S_{ph}, S_{cr}\right)\cdot X, \tag{39} $$

$$ {}_{0}^{FFE}D_{t}^{\alpha,\eta}S_{cr} = D\left(S_{cr0} - S_{cr}\right) - k_{cr}\cdot\mu\left(S_{ph}, S_{cr}\right)\cdot X, \tag{40} $$

$$ {}_{0}^{FFE}D_{t}^{\alpha,\eta}X = -D\beta X + \mu\left(S_{ph}, S_{cr}\right)X \tag{41} $$

The relationship between the fractal derivative and the classical derivative produces:

$$ {}_{0}^{CF}D_{t}^{\alpha}S_{ph} = \eta t^{\eta-1}\left(D\left(S_{ph0} - S_{ph}\right) - k_{ph}\cdot\mu\left(S_{ph}, S_{cr}\right)\cdot X\right), \tag{42} $$

$$ {}_{0}^{CF}D_{t}^{\alpha}S_{cr} = \eta t^{\eta-1}\left(D\left(S_{cr0} - S_{cr}\right) - k_{cr}\cdot\mu\left(S_{ph}, S_{cr}\right)\cdot X\right), \tag{43} $$

$$ {}_{0}^{CF}D_{t}^{\alpha}X = \eta t^{\eta-1}\left(-D\beta X + \mu\left(S_{ph}, S_{cr}\right)X\right) \tag{44} $$

For simplicity, we define

$$ K(t, S_{ph}, S_{cr}, X) = \eta t^{\eta-1}\left(D\left(S_{ph0} - S_{ph}\right) - k_{ph}\cdot\mu\left(S_{ph}, S_{cr}\right)\cdot X\right), \tag{45} $$

$$ L(t, S_{ph}, S_{cr}, X) = \eta t^{\eta-1}\left(D\left(S_{cr0} - S_{cr}\right) - k_{cr}\cdot\mu\left(S_{ph}, S_{cr}\right)\cdot X\right), \tag{46} $$

$$ M(t, S_{ph}, S_{cr}, X) = \eta t^{\eta-1}\left(-D\beta X + \mu\left(S_{ph}, S_{cr}\right)X\right) \tag{47} $$

Then, we obtain

$$ {}_{0}^{CF}D_{t}^{\alpha}S_{ph} = K(t, S_{ph}, S_{cr}, X) \tag{48} $$

$$ {}_{0}^{CF}D_{t}^{\alpha}S_{cr} = L(t, S_{ph}, S_{cr}, X) \tag{49} $$

$$ {}_{0}^{CF}D_{t}^{\alpha}X = M(t, S_{ph}, S_{cr}, X) \tag{50} $$

Applying the CF integral yields [17]:

$$
\begin{aligned}
S_{ph}(t) - S_{ph}(0) = & \quad \frac{1-\alpha}{M(\alpha)} K(t, S_{ph}, S_{cr}, X) + \frac{\alpha}{M(\alpha)} \int_0^t K(\tau, S_{ph}, S_{cr}, X) d\tau \\
S_{cr}(t) - S_{cr}(0) = & \quad \frac{1-\alpha}{M(\alpha)} L(t, S_{ph}, S_{cr}, X) + \frac{\alpha}{M(\alpha)} \int_0^t L(\tau, S_{ph}, S_{cr}, X) d\tau \\
X(t) - X(0) = & \quad \frac{1-\alpha}{M(\alpha)} M(t, S_{ph}, S_{cr}, X) + \frac{\alpha}{M(\alpha)} \int_0^t M(\tau, S_{ph}, S_{cr}, X) d\tau
\end{aligned}
$$

Discretizing the above equations at t_{n+1} and t_n we get:

$$
\begin{aligned}
S_{ph}^{n+1} = & \quad S_{ph}^0 + \frac{1-\alpha}{M(\alpha)} K(t_n, S_{ph}^n, S_{cr}^n, X^n) \\
& + \frac{\alpha}{M(\alpha)} \int_0^{t_{n+1}} K(\tau, S_{ph}, S_{cr}, X) d\tau \\
S_{cr}^{n+1} = & \quad S_{cr}^0 + \frac{1-\alpha}{M(\alpha)} L(t_n, S_{ph}^n, S_{cr}^n, X^n) \\
& + \frac{\alpha}{M(\alpha)} \int_0^{t_{n+1}} L(\tau, S_{ph}, S_{cr}, X) d\tau \\
X^{n+1} = & \quad X^0 + \frac{1-\alpha}{M(\alpha)} M(t_n, S_{ph}^n, S_{cr}^n, X^n) \\
& + \frac{\alpha}{M(\alpha)} \int_0^{t_{n+1}} M(\tau, S_{ph}, S_{cr}, X) d\tau
\end{aligned}
$$

and

$$
\begin{aligned}
S_{ph}^n = & \quad S_{ph}^0 + \frac{1-\alpha}{M(\alpha)} K(t_{n-1}, S_{ph}^{n-1}, S_{cr}^{n-1}, X^{n-1}) \\
& + \frac{\alpha}{M(\alpha)} \int_0^{t_n} K(\tau, S_{ph}, S_{cr}, X) d\tau \\
S_{cr}^n = & \quad S_{cr}^0 + \frac{1-\alpha}{M(\alpha)} L(t_{n-1}, S_{ph}^{n-1}, S_{cr}^{n-1}, X^{n-1}) \\
& + \frac{\alpha}{M(\alpha)} \int_0^{t_n} L(\tau, S_{ph}, S_{cr}, X) d\tau \\
X^n = & \quad X^0 + \frac{1-\alpha}{M(\alpha)} M(t_{n-1}, S_{ph}^{n-1}, S_{cr}^{n-1}, X^{n-1}) \\
& + \frac{\alpha}{M(\alpha)} \int_0^{t_n} M(\tau, S_{ph}, S_{cr}, X) d\tau
\end{aligned}
$$

Thus, we reach

$$
\begin{aligned}
S_{ph}^{n+1} = \quad & S_{ph}^{n} + \frac{1-\alpha}{M(\alpha)}\left(K(t_n, S_{ph}^{n}, S_{cr}^{n}, X^{n}) - K(t_{n-1}, S_{ph}^{n-1}, S_{cr}^{n-1}, X^{n-1})\right) \\
& + \frac{\alpha}{M(\alpha)}\int_{t_n}^{t_{n+1}} K(\tau, S_{ph}, S_{cr}, X)d\tau \\
S_{cr}^{n+1} = \quad & S_{cr}^{n} + \frac{1-\alpha}{M(\alpha)}\left(L(t_n, S_{ph}^{n}, S_{cr}^{n}, X^{n}) - L(t_{n-1}, S_{ph}^{n-1}, S_{cr}^{n-1}, X^{n-1})\right) \\
& + \frac{\alpha}{M(\alpha)}\int_{t_n}^{t_{n+1}} L(\tau, S_{ph}, S_{cr}, X)d\tau \\
X^{n+1} = \quad & X^{n} + \frac{1-\alpha}{M(\alpha)}\left(M(t_n, S_{ph}^{n}, S_{cr}^{n}, X^{n}) - M(t_{n-1}, S_{ph}^{n-1}, S_{cr}^{n-1}, X^{n-1})\right) \\
& + \frac{\alpha}{M(\alpha)}\int_{t_n}^{t_{n+1}} M(\tau, S_{ph}, S_{cr}, X)d\tau
\end{aligned}
$$

Using the two-step Lagrange polynomial yields:

$$
\begin{aligned}
S_{ph}^{n+1} = \quad & S_{ph}^{n} + \frac{1-\alpha}{M(\alpha)}\left(K(t_n, S_{ph}^{n}, S_{cr}^{n}, X^{n}) - K(t_{n-1}, S_{ph}^{n-1}, S_{cr}^{n-1}, X^{n-1})\right) \\
& + \frac{\alpha}{M(\alpha)}\left(\frac{3h}{2}K(t_n, S_{ph}^{n}, S_{cr}^{n}, X^{n}) - \frac{h}{2}K(t_{n-1}, S_{ph}^{n-1}, S_{cr}^{n-1}, X^{n-1})\right) \\
S_{cr}^{n+1} = \quad & S_{cr}^{n} + \frac{1-\alpha}{M(\alpha)}\left(L(t_n, S_{ph}^{n}, S_{cr}^{n}, X^{n}) - L(t_{n-1}, S_{ph}^{n-1}, S_{cr}^{n-1}, X^{n-1})\right) \\
& + \frac{\alpha}{M(\alpha)}\left(\frac{3h}{2}L(t_n, S_{ph}^{n}, S_{cr}^{n}, X^{n}) - \frac{h}{2}L(t_{n-1}, S_{ph}^{n-1}, S_{cr}^{n-1}, X^{n-1})\right) \\
X^{n+1} = \quad & X^{n} + \frac{1-\alpha}{M(\alpha)}\left(M(t_n, S_{ph}^{n}, S_{cr}^{n}, X^{n}) - M(t_{n-1}, S_{ph}^{n-1}, S_{cr}^{n-1}, X^{n-1})\right) \\
& + \frac{\alpha}{M(\alpha)}\left(\frac{3h}{2}M(t_n, S_{ph}^{n}, S_{cr}^{n}, X^{n}) - \frac{h}{2}M(t_{n-1}, S_{ph}^{n-1}, S_{cr}^{n-1}, X^{n-1})\right)
\end{aligned}
$$

As a result, the model's computational scheme for the exponential decay kernel has been discovered. We used this scheme and obtained Figures 5-8.

7. Analysis of the Model with the Mittag-Leffler Kernel

Now we analyze the model with FFD using the Mittag-Leffler kernel as:

$$
{}_{0}^{FFM}D_{t}^{\alpha,\eta}S_{ph} = D\left(S_{ph0} - S_{ph}\right) - k_{ph}\cdot\mu\left(S_{ph}, S_{cr}\right)\cdot X, \tag{51}
$$

$$
{}_{0}^{FFM}D_{t}^{\alpha,\eta}S_{cr} = D\left(S_{cr0} - S_{cr}\right) - k_{cr}\cdot\mu\left(S_{ph}, S_{cr}\right)\cdot X, \tag{52}
$$

$$
{}_{0}^{FFM}D_{t}^{\alpha,\eta}X = -D\beta X + \mu\left(S_{ph}, S_{cr}\right)X \tag{53}
$$

Then, we obtain

$$
\begin{aligned}
{}_{0}^{AB}D_{t}^{\alpha}S_{ph} &= \eta t^{\eta-1}\left(D\left(S_{ph0}-S_{ph}\right)-k_{ph}\cdot\mu\left(S_{ph},S_{cr}\right)\cdot X\right), && (54)\\
{}_{0}^{AB}D_{t}^{\alpha}S_{cr} &= \eta t^{\eta-1}\left(D\left(S_{cr0}-S_{cr}\right)-k_{cr}\cdot\mu\left(S_{ph},S_{cr}\right)\cdot X\right), && (55)\\
{}_{0}^{AB}D_{t}^{\alpha}X &= \eta t^{\eta-1}\left(-D\beta X+\mu\left(S_{ph},S_{cr}\right)X\right) && (56)
\end{aligned}
$$

For simplicity, we define

$$
\begin{aligned}
Y(t,S_{ph},S_{cr},X) &= \eta t^{\eta-1}\left(D\left(S_{ph0}-S_{ph}\right)-k_{ph}\cdot\mu\left(S_{ph},S_{cr}\right)\cdot X\right), && (57)\\
Z(t,S_{ph},S_{cr},X) &= \eta t^{\eta-1}\left(D\left(S_{cr0}-S_{cr}\right)-k_{cr}\cdot\mu\left(S_{ph},S_{cr}\right)\cdot X\right), && (58)\\
T(t,S_{ph},S_{cr},X) &= \eta t^{\eta-1}\left(-D\beta X+\mu\left(S_{ph},S_{cr}\right)X\right) && (59)
\end{aligned}
$$

Then, we get

$$
\begin{aligned}
{}_{0}^{AB}D_{t}^{\alpha}S_{ph} &= Y(t,S_{ph},S_{cr},X), && (60)\\
{}_{0}^{AB}D_{t}^{\alpha}S_{cr} &= Z(t,S_{ph},S_{cr},X), && (61)\\
{}_{0}^{AB}D_{t}^{\alpha}X &= T(t,S_{ph},S_{cr},X) && (62)
\end{aligned}
$$

Applying the AB integral gives,

$$
\begin{aligned}
S_{ph}(t)-S_{ph}(0) &= \frac{1-\alpha}{AB(\alpha)}Y(t,S_{ph},S_{cr},X)+\frac{\alpha}{AB(\alpha)\Gamma(\alpha)}\int_{0}^{t}(t-p)^{\alpha-1}Y(p,S_{ph},S_{cr},X)dp\\
S_{cr}(t)-S_{cr}(0) &= \frac{1-\alpha}{AB(\alpha)}Z(t,S_{ph},S_{cr},X)+\frac{\alpha}{AB(\alpha)\Gamma(\alpha)}\int_{0}^{t}(t-p)^{\alpha-1}Z(p,S_{ph},S_{cr},X)dp\\
X(t)-X(0) &= \frac{1-\alpha}{AB(\alpha)}T(t,S_{ph},S_{cr},X)+\frac{\alpha}{AB(\alpha)\Gamma(\alpha)}\int_{0}^{t}(t-p)^{\alpha-1}T(p,S_{ph},S_{cr},X)dp
\end{aligned}
$$

Discretizing the above equations at t_{n+1}, we get:

$$
\begin{aligned}
S_{ph}^{n+1} = & \quad S_{ph}^{0} + \frac{1-\alpha}{AB(\alpha)} Y(t_{n+1}, S_{ph}^{n}, S_{cr}^{n}, X^{n}) \\
& + \frac{\alpha}{AB(\alpha)\Gamma(\alpha)} \int_{0}^{t_{n+1}} (t_{n+1}-p)^{\alpha-1} Y(p, S_{ph}, S_{cr}, X) dp \\
S_{cr}^{n+1} = & \quad S_{cr}^{0} + \frac{1-\alpha}{AB(\alpha)} Z(t_{n+1}, S_{ph}^{n}, S_{cr}^{n}, X^{n}) \\
& + \frac{\alpha}{AB(\alpha)\Gamma(\alpha)} \int_{0}^{t_{n+1}} (t_{n+1}-p)^{\alpha-1} Z(p, S_{ph}, S_{cr}, X) dp \\
X^{n+1} = & \quad X^{0} + \frac{1-\alpha}{AB(\alpha)} T(t_{n+1}, S_{ph}^{n}, S_{cr}^{n}, X^{n}) \\
& + \frac{\alpha}{AB(\alpha)\Gamma(\alpha)} \int_{0}^{t_{n+1}} (t_{n+1}-p)^{\alpha-1} T(p, S_{ph}, S_{cr}, X) dp
\end{aligned}
$$

Then, we obtain

$$
\begin{aligned}
S_{ph}^{n+1} = & \quad S_{ph}^{0} + \frac{1-\alpha}{AB(\alpha)} Y(t_{n+1}, S_{ph}^{n}, S_{cr}^{n}, X^{n}) \\
& + \frac{\alpha}{AB(\alpha)} \sum_{i=0}^{n} \left[\frac{h^{\alpha} Y(t_i, S_{ph}^{n}, S_{cr}^{n}, X^{n})}{\Gamma(\alpha+2)} \left((n+1-i)^{\alpha} (n-i+2+\alpha) \right. \right. \\
& \qquad \left. \left. -(n-i)^{\alpha} (n-i+2+2\alpha) \right) \right] \\
& - \frac{\alpha}{AB(\alpha)} \sum_{i=0}^{n} \left[\frac{h^{\alpha} Y(t_{i-1}, S_{ph}^{n-1}, S_{cr}^{n-1}, X^{n-1})}{\Gamma(\alpha+2)} \left((n+1-i)^{\alpha+1} \right. \right. \\
& \qquad \left. \left. -(n-i)^{\alpha} (n-i+1+\alpha) \right) \right]
\end{aligned}
$$

$$
\begin{aligned}
S_{cr}^{n+1} = & \quad S_{cr}^{0} + \frac{1-\alpha}{AB(\alpha)} Z(t_{n+1}, S_{ph}^{n}, S_{cr}^{n}, X^{n}) \\
& + \frac{\alpha}{AB(\alpha)} \sum_{i=0}^{n} \left[\frac{h^{\alpha} Z(t_i, S_{ph}^{n}, S_{cr}^{n}, X^{n})}{\Gamma(\alpha+2)} \left((n+1-i)^{\alpha} (n-i+2+\alpha) \right. \right. \\
& \qquad \left. \left. -(n-i)^{\alpha} (n-i+2+2\alpha) \right) \right] \\
& - \frac{\alpha}{AB(\alpha)} \sum_{i=0}^{n} \left[\frac{h^{\alpha} Z(t_{i-1}, S_{ph}^{n-1}, S_{cr}^{n-1}, X^{n-1})}{\Gamma(\alpha+2)} \left((n+1-i)^{\alpha+1} \right. \right. \\
& \qquad \left. \left. -(n-i)^{\alpha} (n-i+1+\alpha) \right) \right]
\end{aligned}
$$

$$
\begin{aligned}
X^{n+1} = & \quad X^0 + \frac{1-\alpha}{AB(\alpha)} T(t_{n+1}, S^n_{ph}, S^n_{cr}, X^n) \\
& + \frac{\alpha}{AB(\alpha)} \sum_{i=0}^{n} \left[\frac{h^\alpha T(t_i, S^n_{ph}, S^n_{cr}, X^n)}{\Gamma(\alpha+2)} \left((n+1-i)^\alpha (n-i+2+\alpha) \right.\right. \\
& \qquad \left.\left. -(n-i)^\alpha (n-i+2+2\alpha) \right) \right] \\
& - \frac{\alpha}{AB(\alpha)} \sum_{i=0}^{n} \left[\frac{h^\alpha T(t_{i-1}, S^{n-1}_{ph}, S^{n-1}_{cr}, X^{n-1})}{\Gamma(\alpha+2)} \left((n+1-i)^{\alpha+1} \right.\right. \\
& \qquad \left.\left. -(n-i)^\alpha (n-i+1+\alpha) \right) \right].
\end{aligned}
$$

Thus, the computational scheme for the model with Mittag Leffler kernel has been obtained. We used this scheme and obtained Figures 9-12.

Remark 1. *The ability to impactively define models for systems with memory impacts is a key and significant advantage of FFD. Fractal-fractional operators with varied memories are related to various non-local dynamical systems' relaxation processes. Models with FFD are therefore more helpful and impactive.*

8. Results and Discussions

This section includes computational simulations for various fractional order and fractal dimension values. We discuss the results with the three different kernels as described in sections 5, 6 and 7. In these figure α, β and η are between zero and one. In these simulations, β is the parameter given on the model, η is fractal dimension and α is the fractional order. In Figure 1, we show the computational simulations for $\beta = 1$ and the fractal dimension $\eta = 1$ for different values of fractional order α with the power-law kernel. In this figure, we can see the impact of the fractional order α. In Figure 2, we show the computational simulations for $\beta = 1$ and the fractal dimension $\eta = 0.8$ for different values of fractional order α with the power-law kernel. In this figure, we can see the impact of the fractional order α. In Figure 3, we show the computational simulations for $\beta = 0.5$ and the fractal dimension $\eta = 1.0$ for different values of fractional order α with the power-law kernel. In this figure, we can see the impact of the fractional order α. In Figure 4, we show the computational simulations for $\beta = 0.5$ and the fractal dimension $\eta = 0.9$ for different values of fractional order α with the power-law kernel. In this figure, we can see the impact of the fractional order α. In Figure 5, we show the computational simulations for $\beta = 1$ and the fractal dimension $\eta = 1$ for different values of fractional order α with the exponential-decay kernel. In this figure, we can see the impact of the

fractional order α. In Figure 6, we show the computational simulations for $\beta = 1$ and the fractal dimension $\eta = 0.7$ for different values of fractional order α with the exponential-decay kernel. In this figure, we can see the impact of the fractional order α. In Figure 7, we show the computational simulations for $\beta = 0.8$ and the fractal dimension $\eta = 1$ for different values of fractional order α with the exponential-decay kernel. In this figure, we can see the impact of the fractional order α. In Figure 8, we show the computational simulations for $\beta = 0.8$ and the fractal dimension $\eta = 0.7$ for different values of fractional order α with the exponential-decay kernel. In this figure, we can see the impact of the fractional order α. In Figure 9, we show the computational simulations for $\beta = 1.0$ and the fractal dimension $\eta = 1.0$ for different values of fractional order α with the Mittag-Leffler kernel. In this figure, we can see the impact of the fractional order α. In Figure 10, we show the computational simulations for $\beta = 1.0$ and the fractal dimension $\eta = 0.5$ for different values of fractional order α with the Mittag-Leffler kernel. In this figure, we can see the impact of the fractional order α. In Figure 11, we show the computational simulations for $\beta = 0.5$ and the fractal dimension $\eta = 1.0$ for different values of fractional order α with the Mittag-Leffler kernel. In this figure, we can see the impact of the fractional order α. In Figure 12, we show the computational simulations for $\beta = 0.5$ and the fractal dimension $\eta = 0.6$ for different values of fractional order α with the Mittag-Leffler kernel. In this figure, we can see the impact of the fractional order α. In these figures, we can also see the impact of the parameter β and the impact of fractal dimension η.

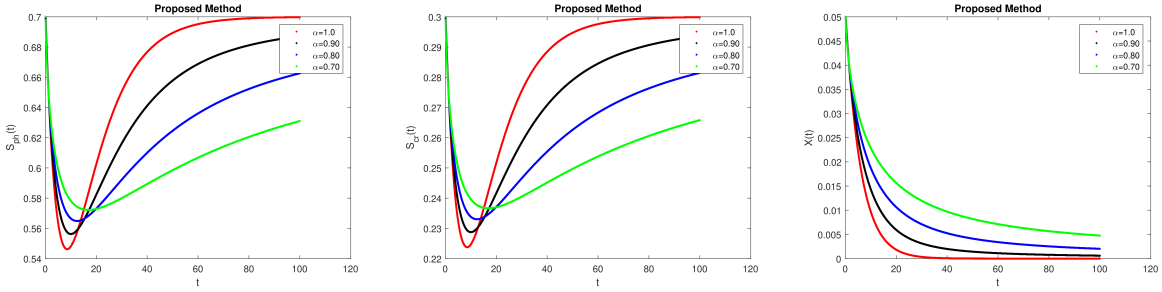

Figure 1: Computational simulations for $\beta = 1$ and the fractal dimension is 1 with the power-law kernel

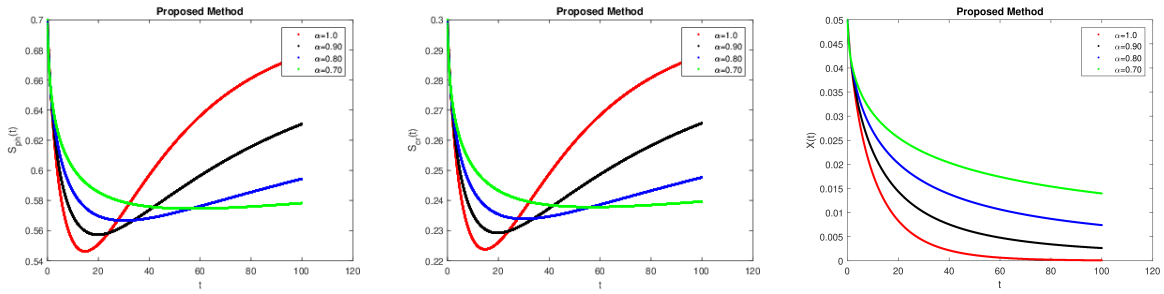

Figure 2: Computational simulations for $\beta = 1$ and the fractal dimension is 0.8 with the power-law kernel

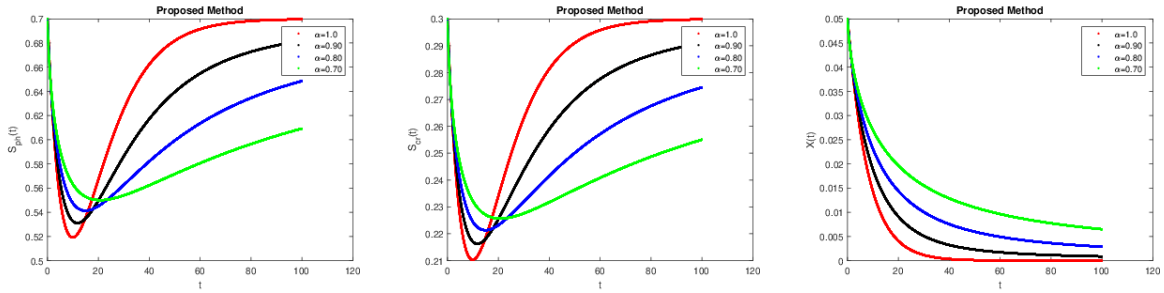

Figure 3: Computational simulations for $\beta = 0.5$ and the fractal dimension is 1 with the power-law kernel

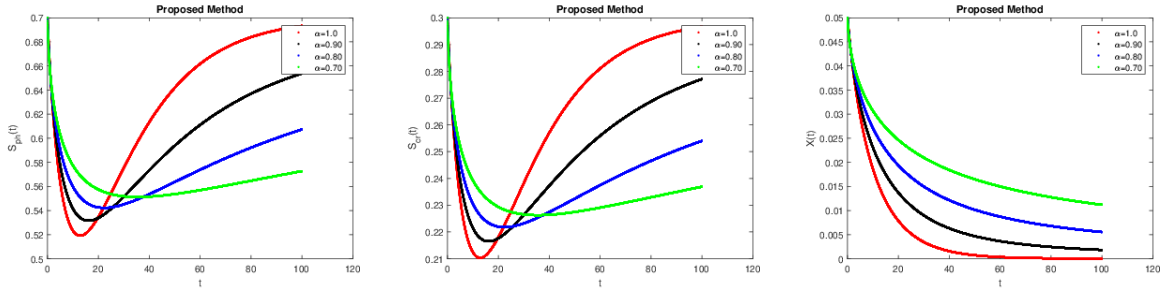

Figure 4: Computational simulations for $\beta = 0.5$ and the fractal dimension is 0.9 with the power-law kernel

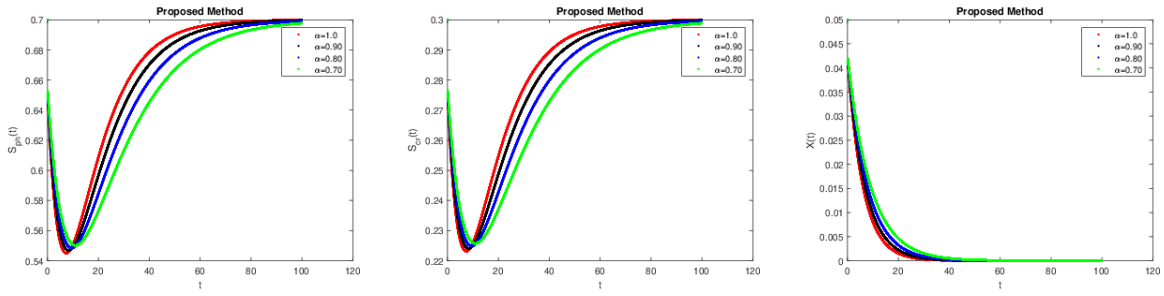

Figure 5: Computational simulations for $\beta = 1.0$ and the fractal dimension is 1 with the exponential-decay kernel

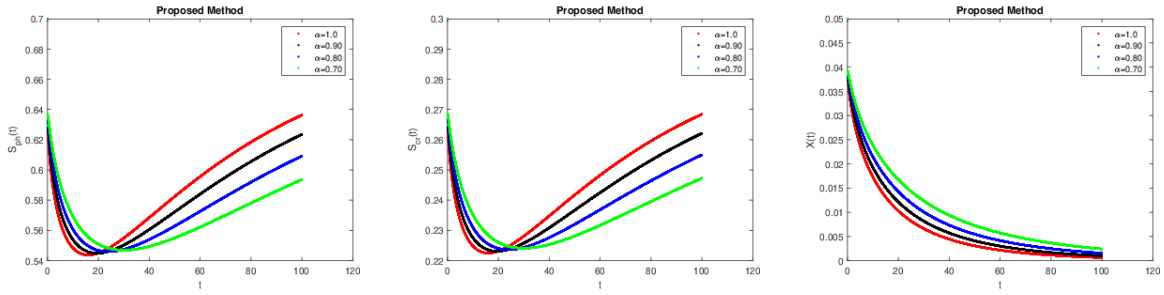

Figure 6: Computational simulations for $\beta = 1.0$ and the fractal dimension is 0.7 with the exponential-decay kernel

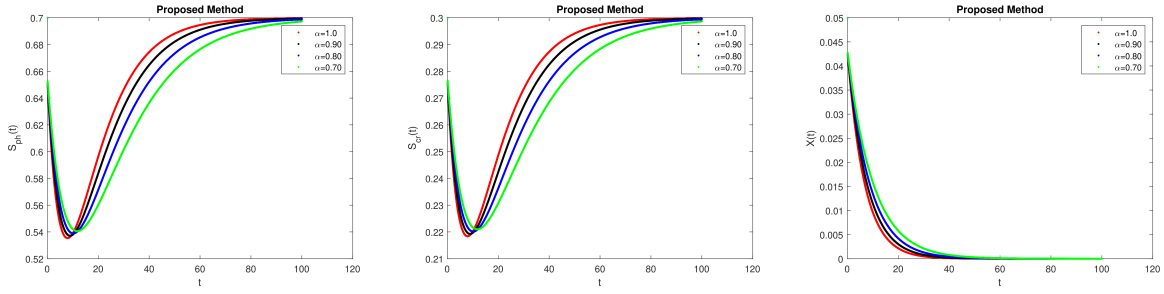

Figure 7: Computational simulations for $\beta = 0.8$ and the fractal dimension is 1.0 with the exponential-decay kernel

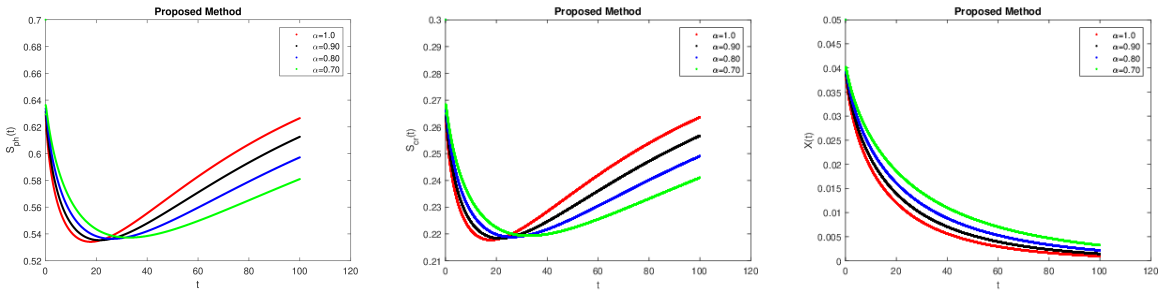

Figure 8: Computational simulations for $\beta = 0.8$ and the fractal dimension is 0.7 with the exponential-decay kernel

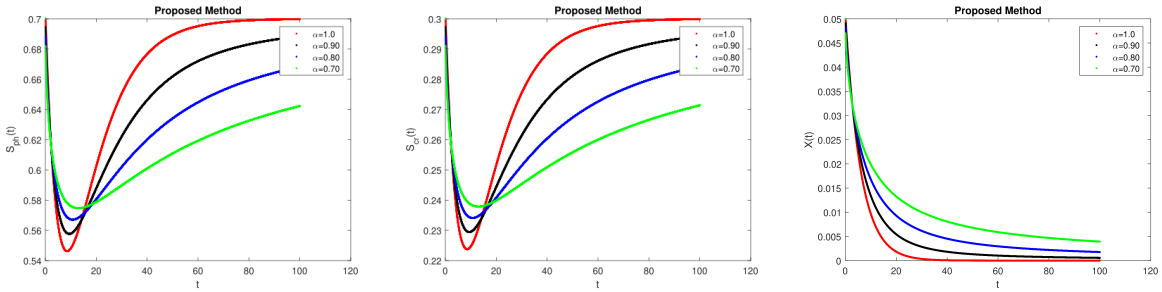

Figure 9: Computational simulations for $\beta = 1.0$ and the fractal dimension is 1.0 with the Mittag-Leffler kernel

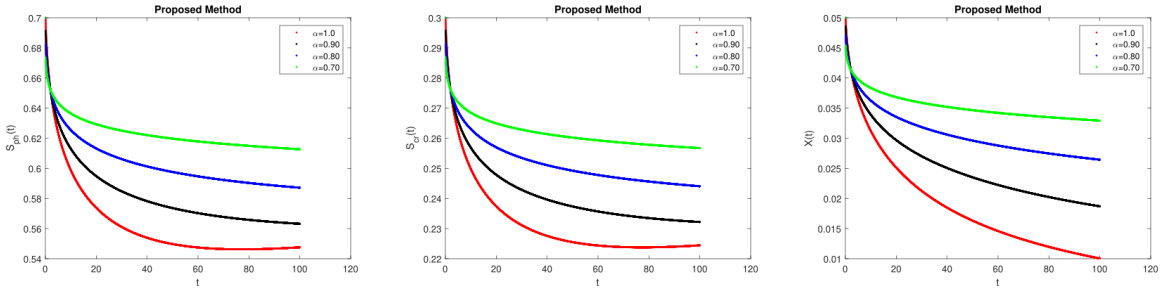

Figure 10: Computational simulations for $\beta = 1.0$ and the fractal dimension is 0.5 with the Mittag-Leffler kernel

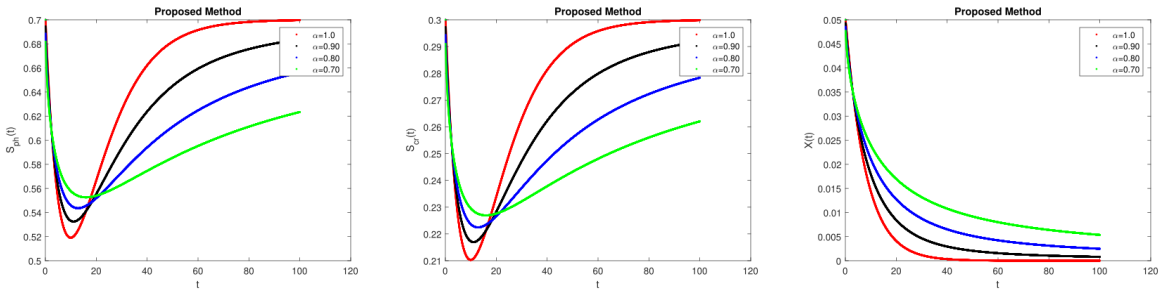

Figure 11: Computational simulations for $\beta = 0.5$ and the fractal dimension is 1.0 with the Mittag-Leffler kernel

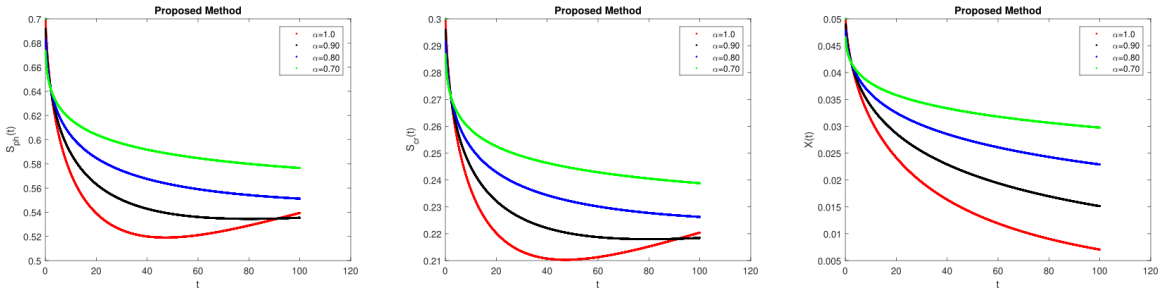

Figure 12: Computational simulations for $\beta = 0.5$ and the fractal dimension is 0.6 with the Mittag-Leffler kernel

9. Conclusion

In a continuously stirred bioreactor, a mathematical model for the breakdown of a phenol and p-cresol mixture was suggested in this manuscript. The model was based on three nonlinear ordinary differential equations. Analysis of their stability and determination of the model's equilibrium points were presented. Utilizing three alternative kernels, we also examined the model with the FFD and looked into the impacts of the fractional order and fractal dimension. For the concentrations of phenol, p-cresol, and biomass, we developed incredibly efficient computational approaches. To demonstrate the accuracy of the suggested technique, we gave the computational simulations for different values of α and β..

Conflict of interest

The authors declare no conflict of interest.

References

[1] N. Dimitrova, P. Zlateva, Global Stability Analysis of a Bioreactor Model for Phenol and Cresol Mixture Degradation. Processes 2021, 9, 124.

[2] J. S. Seo, Y. S. Keum, Q. X. Li, Bacterial degradation of aromatic compounds. Int. J. Environ. Res. Public Health 2009, 6, 278–309. [CrossRef] [PubMed].

[3] N. K. Sharma, L. Philip, S. M. Bhallamudi, Aerobic degradation of phenolics and aromatic hydrocarbons in presence of cyanide. Bioresour. Technol. 2012, 121, 263–273. [CrossRef] [PubMed].

[4] M. C. Tomei, M. C Annesini, Biodegradation of phenolic mixtures in a sequencing batch reactor: A kinetic study. Environ. Sci. Pollut. Res. 2008, 15, 188–195. [CrossRef] [PubMed].

[5] H. Yemendzhiev, P. Zlateva, Z. Alexieva, Comparison of the biodegradation capacity of two fungal strains toward a mixture of phenol and cresol by mathematical modeling. Biotechnol. Biotechnol. Equip. 2012, 26, 3278–3281. [CrossRef].

[6] A. Kietkwanboot, S. Chaiprapat, R. Müller, O. Suttinun, Biodegradation of phenolic compounds present in palm oil mill effluent as single and mixed substrates by Trameteshirsuta AK04. J. Environ. Sci. Heal. Part A Toxic/Hazard. Subst. Environ. Eng. 2020, 55, 989–1002. [CrossRef].

[7] S. Momani, An explicit and computational solutions of the fractional KdV equation. Math. Comput. Simul. 70, No 2 2005, 110–118.

[8] C. Li and J. Cao, A finite difference method for time-fractional telegraph equation, IEEE/ASME International Conference on Mechatronics and Embedded Systems and Applications (MESA), 2012, 314–318.

[9] F. Huang, F. Liu, The fundamental solution of the space-time fractional advection-dispersion equation. J. Appl. Math. Comput. 18, No 1-2 (2005), 21-36.

[10] A.H. Bhrawy, E.H. Doha, S.S. Ezz-Eldien and Robert A. Van Gorder, A new Jacobi spectral collocation method for solving (1 + 1)fractional Schrodinger equations and fractional coupled Schrodinger systems, Eur. Phys. J. Plus (2014) 129: 260.

[11] T. Karatay, S. R. Bayramoglu, A. Sahin, Implicit difference approximation for the time fractional heat equation with the nonlocal condition, Applied Computational Mathematics 61 (2011) 1281–1288.

[12] Y. Chen, M. Yi, C. Chen, C. Yu, Bernstein Polynomials Method for Fractional Convection-Diffusion Equation with Variable Coefficients, CMES, vol.83, no.6, pp.639-653, 2012.

[13] F. Liu, V. Anh, I. Turner, Computational solution of space fractional FokkerPlanck equation. Journal of Computational and Applied Mathematics, vol. 166, pp. 2004, 209 -219.

[14] S. Momani, Z. Odibat, Comparison between the homotopy perturbation method and the variational iteration method for linear fractional partial differential equations. Comput. Math. Appl. 54, No 7-8 (2007), 910–919.

[15] A.M.A. El-Sayed, M. Gaber, The Adomian decomposition method for solving partial differential equations of fractal order in finite domains. Phys. Lett. A. 359, No 3 (2006), 175–182.

[16] A. Atangana, Fractal-fractional differentiation and integration: Connecting fractal calculus and fractional calculus to predict complex, system, Chaos, Solitons and Fractals 102, 2017 396–406.

[17] M. Toufik, A. Atangana, New computational approximation of fractional derivative with non-local and non-singular kernel: application to chaotic models, The European Physical Journal Plus 132 (10), 444.

[18] H. Mohammadi, S. Kumar, Sh. Rezapour, S. Etemad, A theoretical study of the Caputo-Fabrizio fractional modeling for hearing loss due to Mumps virus with optimal control, *Chaos, Solitons and Fractals*, **2021**, 144, 110668. https://doi.org/10.1016/j.chaos.2021.110668

[19] D. Baleanu, A. Jajarmi, H. Mohammadi, Sh. Rezapour, A new study on the mathematical modelling of human liver with Caputo-Fabrizio fractional derivative, *Chaos, Solitons and Fractals*, **2021**, 134, 109705. https://doi.org/10.1016/j.chaos.2020.109705

[20] J. Alzabut, A. Selvam, R. Dhineshbabu, S. Tyagi, M. Ghaderi, Sh. Rezapour, A Caputo discrete fractional-order thermostat model with one and two sensors fractional boundary conditions depending on positive parameters by using the Lipschitz-type inequality, *Journal of Inequalities and Applications*, **2022**, 1–24. https://doi.org/10.1186/s13660-022-02786-0

[21] Z. Heydarpour, J. Izadi, R. George, M. Ghaderi, Sh. Rezapour, On a Partial Fractional Hybrid Version of Generalized Sturm–Liouville–Langevin Equation *Fractal and Fractional*, **2022**, 6(5), 269. https://doi.org/10.3390/fractalfract6050269

[22] R. George, M. Houas, M. Ghaderi, Sh. Rezapour, S. K. Elagan, On a coupled system of pantograph problem with three sequential fractional derivatives by using positive contraction-type inequalities, *Results in Physics*, **2022**, 39, 105687. https://doi.org/10.1016/j.rinp.2022.105687

[23] M. M. Matar, M. I. Abbas, J. Alzabut, M. K. A. Kaabar, S. Etemad, Sh. Rezapour, Investigation of the p-Laplacian nonperiodic nonlinear boundary value problem via generalized Caputo fractional derivatives, *Advances in Difference Equations*, **2021**, 2021:68. https://doi.org/10.1186/s13662-021-03228-9

[24] S. Etemad, I. Avci, P. Kumar, D. Baleanu, S. Rezapour, Some novel mathematical analysis on the fractal-fractional model of the AH1N1/09 virus and its generalized Caputo-type version, *Chaos, Solitons and Fractals*, **2022**, 162, 112511.